Special Section: Soil–Plant–Atmosphere Continuum

Keir Soderberg*
Stephen P. Good
Lixin Wang
Kelly Caylor

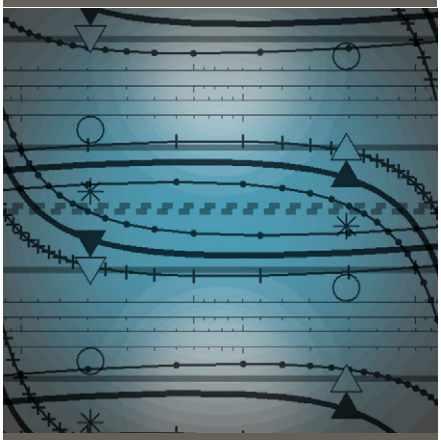

The stable isotopes of soil water vapor can be useful in the study of ecosystem processes. Modeling has historically dominated the measurement of these parameters due to sampling difficulties. We discuss new developments in modeling and measurement, including the implications of including soil water potential in the Craig–Gordon modeling framework.

K. Soderberg, S.P. Good, and K. Caylor, Dep. of Civil and Environmental Engineering, Princeton Univ., Princeton, NJ 08544; L. Wang, Water Research Center, School of Civil and Environmental Engineering, Univ. of New South Wales, Sydney, NSW 2052, Australia, currently at Indiana Univ.–Purdue Univ., Indianapolis (IUPUI), Indianapolis, IN 46202. *Corresponding author (soderbrg@princeton.edu).

Vadose Zone J.
doi:10.2136/vzj2011.0165
Received 15 Nov. 2011.

Stable Isotopes of Water Vapor in the Vadose Zone: A Review of Measurement and Modeling Techniques

The stable isotopes of soil water vapor are useful tracers of hydrologic processes occurring in the vadose zone. The measurement of soil water vapor isotopic composition ($\delta^{18}O$, $\delta^{2}H$) is challenging due to difficulties inherent in sampling the vadose zone airspace in situ. Historically, these parameters have therefore been modeled, as opposed to directly measured, and typically soil water vapor is treated as being in isotopic equilibrium with liquid soil water. We reviewed the measurement and modeling of soil water vapor isotopes, with implications for studies of the soil–plant–atmosphere continuum. We also investigated a case study with in situ measurements from a soil profile in a semiarid African savanna, which supports the assumption of liquid–vapor isotopic equilibrium. A contribution of this work is to introduce the effect of soil water potential (ψ) on kinetic fractionation during soil evaporation within the Craig–Gordon modeling framework. Including ψ in these calculations becomes important for relatively dry soils (ψ < –10 MPa). Additionally, we assert that the recent development of laser-based isotope analytical systems may allow regular in situ measurement of the vadose zone isotopic composition of water in the vapor phase. Wet soils pose particular sampling difficulties, and novel techniques are being developed to address these issues.

Abbreviations: CG, Craig–Gordon.

Soil water dynamics are the part of the hydrologic cycle that is most directly relevant to vegetation dynamics and productivity (e.g., Rodriguez-Iturbe and Porporato, 2004). Measuring the presence, character, and fate of soil water has become standard in agricultural and ecosystem sciences. The stable isotopes of liquid soil water are routinely measured to investigate processes related to plant water uptake such as relative rooting depth (Jackson et al., 1999), recharge rates (Cane and Clark, 1999), and hydraulic redistribution (Dawson, 1993). The isotope values of liquid soil water change in response to fractionation processes such as evaporation and condensation (Gat, 1996) and are thus dynamically linked to the isotope values of the soil water vapor. The isotopic composition of the vapor component of soil water has been much less studied than the liquid water component, mainly due to sampling difficulties. The recent development of laser-based isotope analysis, however, may allow rapid, in situ measurement of soil vapor isotopes. Here we review the measurement and modeling of soil water vapor isotopes, with a focus on the implications of isotope fractionation processes on our understanding of ecohydrology.

The stable isotopic composition of water (δ) is defined as $\delta = ({}^{i}R/{}^{i}R_{std} - 1)$, where ${}^{i}R$ is the ratio of a rare (denoted i, e.g., ^{18}O) to a common isotope ($^{2}H/^{1}H$ or $^{18}O/^{16}O$) in sample water, and ${}^{i}R_{std}$ is the same ratio of the international standard, Vienna standard mean ocean water (VSMOW) (de Laeter et al., 2003; Gonfiantini, 1978). The stable isotope composition of water is a powerful process tracer in ecology, plant physiology, meteorology, and hydrology (e.g., Brunel et al., 1992; Dawson et al., 2002; Gat, 1996; Wang et al., 2010). One of the three landmark studies that were identified in physical meteorology (Lee and Massman, 2011) is about stable isotopes of water. In this study, Craig (1961) discovered a robust relationship between O and H isotopic abundance in precipitation, a relationship now widely known as the global meteoric water line (GMWL), which has become part of the general scientific language today.

The stable isotopic composition of soil water has been used to trace water movement in the unsaturated zone (Barnes and Allison, 1988), estimate the evaporation rate (Allison and

Barnes, 1983), and trace groundwater recharge (Cane and Clark, 1999). The isotopic composition of water in stems and roots usually reflects the isotopic composition of plant-available soil water (Flanagan and Ehleringer, 1991; White et al., 1985), although exceptions can exist in extreme environments (Ellsworth and Williams, 2007). Thus, the isotopic composition of plant stem water has been widely used to identify plant water sources (e.g., irrigation, rainwater, or groundwater) in various ecosystems (Dawson, 1996; Ehleringer and Dawson, 1992; Ehleringer et al., 1999). At the watershed scale, water isotopes can be used to trace catchment water movement and storage mechanisms (Brooks et al., 2010). At the global scale, water isotopes can be used to explore global-scale land–atmosphere interactions (Hoffmann et al., 2000), to reconstruct the past environmental parameters such as ambient temperature and relative humidity (e.g., Helliker and Richter, 2008), and to constrain primary productivity (Welp et al., 2011).

Evaporation from soil, and thus the underlying soil water vapor, can play an important role in the hydrologic cycle, particularly in dryland ecosystems (D'Odorico et al., 2007; Nicholson, 2000; Risi et al., 2010a; Yoshimura et al., 2006). These ecosystems, such as semiarid African savannas, often have significant unvegetated patches and large diurnal and seasonal shifts in temperature and water availability, leading to important feedbacks in vegetation structure (D'Odorico et al., 2007; Nicholson, 2000; Scanlon et al., 2007). For soils in wetter environments, water movement in the liquid phase is more prominent than in the vapor phase, although vapor flux out of the soil could still be a significant component of the water cycle in these environments. These wet soils pose particular vapor sampling difficulties, which are discussed below.

The redistribution of soil water from wetter layers to drier layers at night (hydraulic redistribution) is a widespread phenomenon affecting plant community dynamics and the evaporative flux of soil water (e.g., Feddes et al., 2001; Mooney et al., 1980). In dry soils, however, diurnal shifts in soil temperature gradients can induce the movement of soil water vapor, which flows from warmer to cooler layers where it may condense (Abramova, 1969; Bittelli et al., 2008; Harmathy, 1969; Philip and de Vries, 1957) and become available to plants (Abramova, 1969). This vapor movement can occur in bare soil and have the same effect as hydraulic redistribution. For example, observations of soil water content demonstrated that the movement of water vapor in soils may enhance the ability of *Larrea tridentata* (DC.) Coville to maintain its photosynthesis level at lower soil water potential (Syvertsen et al., 1975) and contribute up to 40% of hourly increases in nocturnal soil moisture within the 15- to 35-cm layer in a seasonally dry ponderosa pine (*Pinus ponderosa* P. Lawson & C. Lawson) forest (Warren et al., 2011). Soil water vapor can also be transported within the soil in response to large gradients in the salt content of the soil (Kelly and Selker, 2001). In extremely dry soils, the intrusion of atmospheric vapor into the upper few centimeters of soil and its condensation can lead to biologically significant increases in the liquid soil water content (Henschel and Seely, 2008).

Land–atmosphere exchange modeling has shown that including a more spatially complex and variable evapotranspiration signal relative to precipitation improves the comparison with observations (Jouzel and Koster, 1996; Yoshimura et al., 2006). Soil water vapor isotopes can help with this parameterization through a combination of measurements and modeling. Due to practical difficulties in sampling, soil evaporation isotopic composition has traditionally been modeled rather than measured. The most commonly used model is the Craig–Gordon (CG) model (Craig and Gordon, 1965; Horita et al., 2008) formulated to estimate equilibrium and kinetic isotopic fractionation during evaporation from the ocean surface. This model has been modified for various applications (Horita et al., 2008), and recently numerical models of isotope flux from the soil have also been developed as alternatives to the CG model (Braud et al., 2005a, 2009b; Haverd and Cuntz, 2010; Mathieu and Bariac, 1996; Melayah et al., 1996a). Comparisons among measured and modeled values of soil evaporate isotopic composition have shown significant deviations from the CG model (Braud et al., 2009a; Haverd et al., 2011; Rothfuss et al., 2010).

Measurement

Measurements of soil water vapor isotopic composition are scarce (Braud et al., 2009b; Haverd et al., 2011; Mathieu and Bariac, 1996; Rothfuss et al., 2010; Stewart, 1972; Striegl, 1988) due to sampling difficulties. Table 1 lists measurement and modeling methods and relevant references.

Water Vapor Sampling and Isotope Analysis

The traditional "cold trap" sampling technique for isotope analysis of water vapor involves drawing air through a tube immersed in a dry ice–alcohol mixture (for H_2O) or liquid N_2 (for H_2O and CO_2), where the water freezes (Dansgaard, 1953; Pollock et al., 1980; Yakir and Wang, 1996). The method has been optimized for efficiency, bringing sampling times below 15 min depending on the humidity level (Helliker et al., 2002), and for portability (Peters and Yakir, 2010). Another recent approach has been the use of a molecular sieve to trap water vapor quantitatively, from which the collected sample is distilled in the laboratory (Han et al., 2006). The water sample then undergoes preparation and analysis—most commonly via isotope ratio mass spectrometry after equilibration with CO_2 for $\delta^{18}O$ determination and reduction via Zn or U for $\delta^{2}H$ determination, although there are many alternative preparation and sample introduction techniques as well as new optical analytical methods available (de Groot, 2009).

Cryogenic sampling of atmospheric water vapor has been performed at various scales since the first vertical profile collections in the 1960s over North America and Europe, which included sampling in both troposphere and stratosphere (Araguás-Araguás et al., 2000; Pollock et al., 1980; Rozanski, 2005). Near-surface cryogenic atmospheric water vapor sample collections have been performed in Europe, Asia, Brazil, and Israel (Risi et al., 2010b; Rozanski, 2005; Twining et

Table 1. Summary of measurement and modeling techniques to quantify isotopic compositions of soil water vapor and soil evaporation.

Potential methods	Notes	References
Measurement		
Isothermal equilibrium (H_2O, CO_2, H_2)†	inside the laboratory	Stewart (1972), Scrimgeour (1995), Hsieh et al. (1998), Richard et al. (2007), Wassenaar et al. (2008)
In situ CO_2–H_2O equilibrium†	in the vadose zone	Hesterberg and Siegenthaler (1991), Hsieh et al. (1998),Tang and Feng (2001), Wingate et al. (2008)
Cryogenic soil column vapor collection	inside the laboratory	Zimmerman et al. (1967), Stewart (1972), Braud et al. (2009a, 2009b), Rothfuss et al. (2010)
In situ cryogenic soil gas sampling	in the vadose zone	Striegl (1988), references in Mathieu and Bariac (1996)
In situ sealed chamber	from soil surface	Haverd et al. (2011)
Open chamber with mass balance	from soil surface	Wang et al. (2012)
In situ direct measurement with laser spectroscopy	in the vadose zone	this study
Modeling		
Craig–Gordon model	formulated for free water evaporation	Craig and Gordon (1965), Horita et al. (2008)
Analytical isotope transport models		Zimmerman et al. (1967), Barnes and Allison (1983)
Numerical isotope transport models	varied results but capture the shape of observations well	Shurbaji and Phillips (1995), Mathieu and Bariac (1996), Melayah et al. (1996a, 1996b), Braud et al. (2005a, 2005b), Braud et al. (2009a, 2009b), Haverd and Cuntz (2010), Haverd et al. (2011)

† These methods are used to estimate liquid soil water isotopic composition, but the details of the equilibrium and sampling methods are relevant to soil water vapor isotopes.

al., 2006; Yamanaka and Shimizu, 2007; Yu et al., 2005), with one group making routine collections since the early 1980s at a surface collection station in Heidelberg, Germany (Jacob and Sonntag, 1991; Rozanski, 2005).

With the development of relatively portable laser isotope analyzers (Kerstel et al., 1999), many airborne and ground-based measurements of $\delta^{18}O$ and $\delta^{2}H$ have been made (Griffis et al., 2010; Hanisco et al., 2007; Lee et al., 2005; Webster and Heymsfield, 2003). The laser isotope instrumentation allows direct, rapid (1–10 Hz) determination of water vapor isotopic composition, with uncertainties approaching those of traditional mass spectrometric methods (de Groot, 2009; Wang et al., 2009). There are now also remote sensing technologies that produce water isotope data for the atmosphere (Worden et al., 2007), and ground-based Fourier transform infrared spectroscopy is developing into a source of this information for the lower troposphere (Schneider et al., 2010).

Soil Water Vapor Sampling and Isotope Analysis

Sampling of soil water vapor has been performed in the past using soil gas sampling apparatus and, as with atmospheric water vapor, cryogenic traps either in the laboratory (Stewart, 1972) or the field (Mathieu and Bariac, 1996; Striegl, 1988). The pioneering work of Zimmerman et al. (1967) on evaporative enrichment in liquid soil water isotopes included an apparatus that directly collected the vapor resulting from soil evaporation, but this condensed vapor was not analyzed. Soil gas sampling via pumping is routinely performed during the monitoring and remediation of organic solvent contamination of the subsurface. The solvent sampling and pumping devices, however, are not designed for the high concentrations and low vapor pressures that characterize soil water vapor relative to organic solvents (e.g., trichloroethylene). The vadose zone modeling efforts surrounding soil gas sampling, however, can help in estimating the area of influence for a given pumping rate and time span. For example, the USGS modeling framework MODFLOW now has a module for vadose zone gaseous transport (Panday and Huyakorn, 2008).

The main concern in the sampling of soil water vapor for isotope analysis is the fractionation of the original isotopic composition through (i) inducing evaporation of the liquid soil water during sampling, and (ii) condensing vapor inside the sampling apparatus due to the typically saturated conditions of soil water vapor (Campbell and Norman, 1998). An approach to reduce the risk of inducing evaporation is to pump at low flow rates (<200 mL min^{-1}), which has produced reasonable results during initial testing (see the case study in the African savanna below). Condensation in the sampling apparatus is reduced by minimizing the tubing length, using all Teflon or high-density polyethylene materials on wettable surfaces, and insulating or even heating the tubing if necessary (Griffis et al., 2010). In wet soils, various membranes could be used to exclude liquid water from the sampling apparatus up to a certain level of pore space saturation. Once the soils reach a low air-filled porosity level, however, authentic vapor sampling becomes impossible. At this critical level, which still needs to be determined empirically for each sampling method and soil type, liquid–vapor equilibrium needs to be assumed and the liquid itself analyzed. In a novel approach

aimed at estimating this liquid soil water isotopic composition in situ, a membrane contactor (Membrana) has been shown to provide reliable results across a fairly wide soil temperature range (8–21°C) through the controlled evaporation of liquid soil water (Herbstritt et al., 2012).

There are two methods for estimating the liquid soil water isotopic composition that are related to soil water vapor sampling. They involve sampling and analyzing CO_2 or water vapor that is in isotopic equilibrium with the liquid soil water. The CO_2 sampling method is based on isotope equilibrium between the soil CO_2 and liquid soil water (Scrimgeour, 1995), which has been shown to be complete below the depth of atmospheric CO_2 invasion into the soil surface (Wingate et al., 2009). This depth of invasion was found to be shallower than 5 cm in Mediterranean soils (Wingate et al., 2009), which is consistent with other investigations that found good agreement between liquid soil water and CO_2 at their shallowest depths: 20 cm (Tang and Feng, 2001) and 30 cm (Hesterberg and Siegenthaler, 1991). Interestingly, although the uncatalyzed equilibrium reaction between CO_2 and H_2O reaches equilibrium in about 3 h (Dansgaard, 1953), the enzyme carbonic anhydrase acts as a catalyst in both plant leaves and soil, such that the $\delta^{18}O$ of CO_2 is a good tracer of photosynthetic and respiratory CO_2 exchange with the atmosphere (Wingate et al., 2009). It is not clear whether soil water vapor plays a significant role in this reaction, but a calculation by Hsieh et al. (1998) estimated the added uncertainty due to reactions between different phases of water in the soil at 0.36‰ for $\delta^{18}O$. The sampling method for CO_2 is either with a chamber placed above the soil surface (e.g., Wingate et al., 2008) or a tube buried in the ground (Tang and Feng, 2001).

The second equilibration method involves placing a soil sample in a sealed plastic bag, filling the bag with dry air, and allowing the atmosphere inside the bag to reach 100% relative humidity at a constant temperature (Wassenaar et al., 2008). The bag is then punctured with a syringe connected directly to a laser isotope analyzer, the vapor is analyzed directly, and its isotopic composition is used along with the equilibration temperature to calculate the soil liquid isotopic composition. This method is instructive with respect to the rate of equilibration between liquid and vapor phases—from 10 min (free water) to 3 d (clay) at 22°C—as well as the time for the laser isotope analyzer to provide a stable signal (~300 s with a flow rate of ~150 mL min^{-1} and a headspace of ~900 mL). For comparison with equilibration in the field, a study in the volcanic soils of Hawaii estimated an in situ equilibration time of 48 h between the $\delta^{18}O$ of liquid soil water and soil CO_2 (Hsieh et al., 1998). Another interesting aspect of the plastic bag equilibration method is that below 5% volumetric water content, the data were apparently not useable even though the headspace reached 100% relative humidity. This method is similar to direct equilibration of soils and plants with CO_2 and H_2 in the laboratory (Scrimgeour, 1995), which was proposed as a good method for obtaining results for very dry samples (<0.5 mL of water).

A comparison among CO_2 equilibration, vacuum distillation, and azeotropic distillation found fair agreement among the methods but also showed distinctly poor results for the CO_2 method in samples drier than about 5% moisture content (Hsieh et al., 1998). The equilibration methods for liquid soil water are potentially quite useful in studies of plant xylem and transpired water isotopic composition in that they could provide a better representation of plant-available water than vacuum and chemical distillation methods, which are performed at elevated temperatures and thus can access more tightly bound water in the soil (Araguás-Araguás et al., 1995; Hsieh et al., 1998; Walker et al., 1994). Further studies are needed, however, to relate soil water held at various water potentials to plant water uptake (e.g., Brooks et al., 2010), liquid–vapor equilibration times, and liquid–vapor fractionation factors.

Measuring the Isotopic Composition of Soil Evaporation

The isotopic composition of soil evaporation can be estimated through sampling the water vapor above the soil. Measurements of the near-surface atmosphere have been used for this purpose to measure vapor efflux from terrestrial ecosystems, including the "Keeling plot" approach using gradients in the isotopic composition and bulk concentration of CO_2 (Keeling, 1958), which has also been applied to water vapor (Wang et al., 2010; Yakir and Sternberg, 2000; Yepez et al., 2003). Additional methods include the flux gradient (Griffis et al., 2004; Yakir and Wang, 1996) and eddy covariance techniques (Griffis et al., 2010; Lee et al., 2005). Each of these methods involves making measurements at some altitude above the ground surface, and thus their results are applicable to a certain horizontal "footprint" from which the vapor originated. If this footprint is unvegetated, then the water vapor flux signal can be completely attributed to soil evaporation. If there is some vegetation present, however, the measured flux is from the combined evapotranspiration. Decomposing this combined signal is possible (Haverd et al., 2011; Rothfuss et al., 2010; Wang et al., 2010), but the assumptions involved in estimating the transpiration and evaporation end members currently lead to a high degree of uncertainty (Good et al., 2012). Specifically, the isotopic end member for transpiration represents an integrated signal weighted by the amount of transpired water delivered by each root of each transpiring plant with the active flux footprint. If the mean rooting depth changes (e.g., grasses become active), the transpiration end member will change. Thus, characterizing this end member with time requires regular measurement of soil water isotopic composition profiles in a way that captures heterogeneity across the footprint, as well as measurement of the transpiring leaf area for plant groups with differing rooting depths (e.g., grasses, shrubs, and trees). Numerical models of soil evaporation isotopic composition, discussed below, coupled with land surface dynamic models have made some advances in this field (Braud et al., 2009a; Haverd et al., 2011).

Another method for measuring soil efflux involves placing a sealed chamber over the soil and measuring the vapors that move up into

the chamber (Haverd et al., 2011; Wingate et al., 2008). The issues with this type of measurement include making a good seal with the soil surface to avoid drawing in atmospheric air, and altering the ambient conditions of the soil. If these sources of error can be minimized, chamber methods have the potential to provide good point estimates of CO_2 and H_2O releases from the soil. Chamber measurements are still challenging, however, because they necessarily change the ambient conditions, especially with respect to wind velocities and concentration gradients for the gases of interest. Improvements are still being made, particularly with open-chamber methods (Midwood et al., 2008) and open-path isotopic composition sensors (Humphries et al., 2010).

Point estimates, however, whether from chamber methods, sampling, or in situ measurements, must be viewed with caution given the typically large degree of heterogeneity in a soil landscape (Ogée et al., 2004). For this reason, integrated landscape-scale estimates of soil evaporation will be more useful for investigating overall ecosystem functioning. Thus increasing the size of an atmospheric measurement's footprint can increase its relevance for scaling up to regional and global levels. The next step toward understanding the distribution of the soil evaporation isotopic composition across a wider range of temporal and spatial scales is modeling based on more readily available data (Braud et al., 2009a; Haverd et al., 2011) and improved mechanistic understanding (e.g., the effect of water potential on the soil evaporation isotopic composition as proposed below).

Modeling Soil Water Vapor Isotopic Composition

Modeling efforts relating to the soil water vapor isotopic composition (δ_V) have focused on estimating the isotopic composition of soil evaporation (δ_E), with reference to the fractionation that occurs during the evaporation of liquid soil water (δ_L). The δ_E modeling has typically been performed in the framework of open-water evaporative fractionation developed by Craig and Gordon (1965), and recently numerical isotope transport models have been developed as an alternative (Braud et al., 2005a, 2009a; Haverd and Cuntz, 2010; Mathieu and Bariac, 1996; Melayah et al., 1996a; Shurbaji and Phillips, 1995).

Liquid–Vapor Equilibrium Isotopic Fractionation

Every isotope fractionation model relies on estimates of the liquid–vapor equilibrium fractionation factors $\alpha_{e,L/V}(^{18}O)$ and $\alpha_{e,L/V}(^{2}H)$:

$$\alpha_{e,L/V}\left(^{18}O\right)=\frac{^{18}R_L}{^{18}R_V} \qquad [1]$$

These parameters change under different environmental conditions. Temperature is the environmental parameter used for the $\alpha_{e,L/V}$ estimates, and this relationship ($\alpha_{e,L/V}$–T) has been well characterized experimentally (Horita and Wesolowski, 1994; Majoube, 1971). Efforts to model the underlying processes of the $\alpha_{e,L/V}$–T relationship from theory (Chialvo and Horita, 2009; Oi, 2003) have not improved on the empirical relationships that have been implemented in studies of evaporation for more than four decades (Horita et al., 2008). Thermodynamic modeling based on equations of state for various water molecule isotopoloques captures the purely empirical relationships well (Japas et al., 1995; Polyakov et al., 2007). The $\alpha_{e,L/V}$–T relationship has only been modified slightly since Majoube (1971) to cover a larger temperature range (Horita and Wesolowski, 1994), with the current formulations given as

$$10^3 \ln\alpha_{e,L/V}\left(^{18}O\right)=-7.685+6.7123\left(\frac{10^3}{T}\right)-1.6664\left(\frac{10^6}{T}\right)+0.35041\left(\frac{10^9}{T}\right) \qquad [2]$$

$$10^3 \ln\alpha_{e,L/V}\left(^{2}H\right)=1158.8\left(\frac{T^3}{10^9}\right)-1620.1\left(\frac{T^2}{10^6}\right)+794.84\left(\frac{T}{10^3}\right)-161.04+2.9992\left(\frac{10^9}{T^3}\right) \qquad [3]$$

where T is the water temperature (K).

Three modeling approaches using (i) molecular simulation, (ii) theoretical (ab initio) calculations, and (iii) thermodynamics have recently been compiled to examine the effects of isotopic substitutions on the properties of the water molecule (Chialvo and Horita, 2009). These three approaches capture the shape of the observed $\alpha_{e,L/V}$–T relationships (Eq. [2] and [3]), but the difference among the models is large relative to the level of fractionation seen empirically (Table 2). Molecular modeling is used by chemists as a supplement to experimentation in an effort to understand the underlying dynamics in chemical reactions. Various modeling approaches are used to depict electron densities and molecular orbital dynamics based on energies associated with all bonded and unbonded atomic interactions.

Using molecular-based simulation, $\alpha_{e,L/V}$ was estimated based on two contrasting models of the water molecule: Gaussian charge polarizable (GCP) and nonpolarizable extended simple point charge (SPC/E). The GCP model performed better than SPC/E but produced fractionation factors ($\alpha_{e,L/V}$) around 5‰ higher for $\alpha_{e,L/V}(^{18}O)$ and 500‰ higher for $\alpha_{e,L/V}(^{2}H)$ than those $\alpha_{e,L/V}$ values found experimentally at 25°C (Horita and Wesolowski, 1994; Majoube, 1971). Chialvo and Horita (2009) recognized the large

Table 2. Liquid–vapor isotopic fractionation factors $\alpha_{L/V}(^{18}O)$ and $\alpha_{L/V}(^{2}H)$ for water (see Horita et al., 2008, for compiled historical values). Equilibrium values are listed for 25°C unless noted. Italics indicate modeled values.

Method	$\alpha_{L/V}(^{18}O)$	$\alpha_{L/V}(^{2}H)$	Description	Reference
Equilibrium				
Best current values (empirical)	1.009347	1.07875	combination of evaporation experiments	Horita and Wesolowski (1994)
Ab initio	*1.008*†	*1.107*	HF calculation level	Oi (2003)
Ab initio	*1.013*	*1.145*	B3LYP calculation level	Oi (2003)
Molecular simulation	*1.016*	*1.622*	Gaussian charge polarizable	Chialvo and Horita (2009)
Molecular simulation	*1.018*	*1.612*	nonpolarizable extended simple point charge	Chialvo and Horita (2009)
Thermodynamics	*1.00935*	*1.0798*	corresponding states principle	Japas et al. (1995), Polyakov et al. (2007)
Empirical, dried clay	NA‡	1.04§	vapor equilibrium with KCl solution	Stewart (1972)
Empirical, silica tubes	NA	1.055¶	vapor equilibrium, variable relative humidity	Richard et al. (2007)
Kinetic (D/D_i):				
Best current values (empirical)	1.0285	1.0251	evaporation at 20°C in air	Merlivat (1978)
	1.0281	1.0249	evaporation at 20°C in N_2	Merlivat (1978)
Recent experiment	1.0275	1.0230	values from the 20.1°C experiment in air	Luz et al. (2009)
Gas kinetic theory	*1.0323*	*1.0166*	in dry air; isotopologues have identical collision diameters	Horita et al. (2008)
Gas kinetic theory	*1.0319*	*1.0164*	in N_2; isotopologues have identical collision diameters	Cappa et al. (2003)

† All equilibrium model values (ab initio, molecular dynamic, and thermodynamic) estimated from Chialvo and Horita (2009, Fig. 4, 6, and 8).
‡ NA, not available.
§ Temperature unknown, listed as "room temperature"; the listed $\alpha_{L/V}(^{2}H)$ value (1.04) is the median of 0.93 to 1.06 ($n = 7$).
¶ Temperature was 20°C rather than 25°C. The free water $\alpha_{L/V}(^{2}H)$ value at 20°C is 1.08453 from Eq. [3]. The listed value (1.055) was the maximum observed, corresponding to relative humidity (RH) values above ~70%. Lower RH conditions corresponded to lower values of $\alpha_{L/V}(^{2}H)$ down to around 1.30 at 10% RH.

deviations of their models from experimental data and suggested a parameterization of their $\alpha_{e,L/V}$–T relationship that would allow experimental data to create more accurate molecular dynamics models in the future. Two ab initio ("from first principles") models using molecular orbital calculations performed somewhat better relative to empirical data, within 4‰ for $\alpha_{e,L/V}(^{18}O)$ and 66‰ for $\alpha_{e,L/V}(^{2}H)$ (Oi, 2003).

Lastly, two thermodynamic modeling efforts produced much better results applying solute dissolution (Japas et al., 1995) and corresponding states principle (Polyakov et al., 2007) approaches, apparently with deviations from empirical data of <0.1 and 1‰ for $\alpha_{e,L/V}(^{18}O)$ and $\alpha_{e,L/V}(^{2}H)$, respectively, at typical environmental temperatures. Despite their different approaches, these two thermodynamic models show very good agreement with each other, especially below 50°C. These approaches do incorporate some empirical data—e.g., vapor pressures for solutions of pure isotopically substituted water (D_2O and $H_2{}^{18}O$).

Overall, the somewhat empirical thermodynamic modeling (Japas et al., 1995; Polyakov et al., 2007) performed much better than the purely theoretical ab initio (Oi, 2003) and molecular simulation (Chialvo and Horita, 2009) models. Most importantly, all three approaches, in spite of drastic differences in $\alpha_{e,L/V}$, show the same shape and limit characteristics. Therefore these models have the potential to provide insight into the underlying mechanisms of the robust empirical $\alpha_{e,L/V}$–T relationships (Eq. [2] and [3]), which are still preferred for estimating $\alpha_{e,L/V}$ (Gat, 1996; Horita et al., 2008; Kim and Lee, 2011).

Isotopic Fractionation during Evaporation from Free Water

The empirical $\alpha_{e,L/V}$ values discussed above can be used to calculate the isotopic composition of vapor that is in isotopic equilibrium with liquid water at a given temperature. This equilibrium is probably reached in soil pore spaces where sufficient moisture is available (Braud et al., 2005a, 2005b; Mathieu and Bariac, 1996), as is illustrated with a case study below. The fractionation during evaporation from a free surface (e.g., the ocean) involves both equilibrium (α_e) and kinetic (α_k) fractionation, and is described here as a basis for the soil evaporation discussion that follows.

Modeling efforts that include both equilibrium and kinetic fractionation were motivated by early observations of marine water vapor being isotopically depleted relative to the equilibrium fractionation factor for a given temperature (Craig and Gordon, 1965). Thus, in addition to $\alpha_{e,L/V}$ for a given temperature at the evaporating surface (T_0), the parameters required for the estimation of the kinetic fractionation include relative humidity (h), diffusivity ratios of the isotopologues of interest (D/D_i), and an aerodynamic parameter (n, Table 3). The variability in these kinetic parameters is dominated by the relative humidity of the air into which the water is evaporating (h_A),

Table 3. Craig–Gordon model parameters and example calculations of the isotope values of the evaporate δ_E for free water and soil water. The example depth data were collected on 29 Mar. 2011 at Mpala Research Center, Kenya, from a soil profile fitted with buried Teflon tubing from which air was drawn directly into a water vapor isotope analyzer (DLT-100, Los Gatos Research). See Appendix for parameter definitions.

Parameter	Mean of 5-, 10-, 20-, and 30-cm depths		5-cm depth		Typical range	
T_A, K	302		302		280–310	
T_0, K	300		301		290–320	
h_A	0.331		0.331		0.2–0.6	
$h_A'(T)$	0.374		0.351		0.2–1.0	
$h_A'(T,\psi)$	0.429		0.433			
ψ_0, MPa	−18.8		−29.2		−1 to −100	
θ_0 (v/v)	0.0602		0.0525		0.01–0.45	
θ_s (v/v)	0.45		0.45		0.2–0.5	
θ_r (v/v)	0.035		0.035		0.01–0.05	
Depth min., cm	5		5		10–50†	
Depth max., cm	30		5			
n (θ)	0.970		0.979		0.5–1.0	
n (free water)	0.5		0.5		0.5	
	$\delta^{18}O$	δ^2H	$\delta^{18}O$	δ^2H	$\delta^{18}O$	δ^2H
$\alpha_{e,L/V}$	1.009206	1.07693	1.009117	1.07579	1.008–1.010	1.059–1.088
D/D_i	1.0285	1.0251	1.0285	1.0251	1.028–1.032	1.016–1.025
$\varepsilon_{k,L/V}(\theta,T)$	0.01728	0.01523	0.01810	0.01596	0.001–0.023	0.001–0.020
$\varepsilon_{k,L/V}(\theta,T,\psi)$	0.01578	0.01391	0.01581	0.01394		
$\varepsilon_{k,L/V}$(free water,T)	0.00891	0.00786	0.00925	0.00815	0.001–0.014	0.001–0.013
r_m/r	1	1	1	1	0.5–1.0	0.5–1.0
δ_L	6.2‡	6.5	13.2	26.2	−5 to 10	−30 to 30
δ_V(meas)	−2.8	−56.6	−2.2	−54.6	NA§	NA
δ_V(equil)	−3.0	−65.4	4.1	−46.1	−15 to 3.0	−120 to −30
δ_A	−10.4	−68.7	−10.4	−68.7	−10 to −20	−50 to −150
Calculated evaporate						
$\delta_E(\theta,T)$	−25.6	−94.3	−15.7	−65.1		
$\delta_E(\theta,T,\psi)$	−24.5	−94.6	−12.6	−61.3		
δ_E(free water,T)	−12.7	−83.7	−2.5	−54.0		

‡ All isotope values are presented here in per-mil notation ($\delta \times 1000$), whereas in calculations they were converted to decimal notation (e.g., Eq. [4], resulting in −25.6‰ for $\delta_E(\theta,T)$ in Column 2 above: $d_E = [(0.0062/1.009206) - 0.374(-0.0104) - 0.009206 - 0.01728]/(1 - 0.374 + 0.01728) = -0.0256$).
† Typical evaporating front depth from Barnes and Allison (1988).
§ NA, not available.

which must be recalculated (h_A') from the measured value at some height above the evaporating surface based on the temperature and activity of water (a_w) at the evaporating surface (Craig and Gordon, 1965; Horita, 2005; Horita et al., 2008; Sofer and Gat, 1975). The overall relationship was first described by Craig and Gordon (1965) and is still used to estimate isotopic fractionation during evaporation from both a free surface and soil (Gat, 1996; Horita et al., 2008):

$$\delta_E = \frac{\delta_L/\alpha_{e,L/V} - h_A'\delta_A - (\alpha_{e,L/V} - 1) - \varepsilon_{k,L/V}}{1 - h_A' + \varepsilon_{k,L/V}} \quad [4]$$

$$\varepsilon_{k,L/V} = n\left(1 - h_A'\right)\left(\frac{D}{D_i} - 1\right)\frac{r_m}{r} \quad [5]$$

$$h_A' = \frac{h_A e_{sA}}{a_w e_{s0}} \quad [6]$$

where e_{sA} and e_{s0} are the saturation vapor pressures at the atmospheric air temperature and the temperature of the evaporation surface, respectively. See the Appendix for full parameter descriptions with units. The weighting term r_m/r is assumed to be 1 for small

water bodies, but can reach 0.5 for strongly evaporating systems like the Mediterranean Sea (Gat, 1996). As summarized in Horita et al. (2008), the CG model is a physically based model where the air–water interface is at isotopic equilibrium. Above this interface is a laminar flow layer of variable thickness, which accounts for additional fractionation due to differences in the molecular diffusivities of isotopologues. This laminar layer is followed by a turbulent mixing layer, which does not contribute to isotope fractionation. The effect of the aerodynamic parameter n ($n = 0.5$ for free water, 1 for completely laminar flow as in very dry soil, see below) is to reduce the kinetic fractionation due to the reduced role of molecular diffusion when the turbulent layer interacts strongly with the evaporating surface. Higher humidity leads to reduced kinetic fractionation, but its overall effect on δ_E is not straightforward because an increased h_A' leads to both a lower numerator and a lower denominator in Eq. [4]. Interestingly, the thermodynamic activity of water (a_w, between ~0.6 in brines to 1 in fresh water) acts to increase the normalized humidity h_A' for evaporation from saline water. The same is true for evaporation from soils, as introduced below, when the soil water potential is used to calculate the activity of soil water. Thus, a reduced activity of water leads to limited evaporative enrichment in saline water relative to fresh water exposed to the same conditions (Horita, 2005). The necessary field measurements to make a CG calculation are discussed below with the case study. The appropriate height for making the atmospheric measurements is above the turbulent mixing layer, given that these values are meant to represent the "free atmosphere" (Craig and Gordon, 1965; Horita et al., 2008), although this condition is probably not fully satisfied for many applications of the CG model.

In addition to normalized humidity, the representation of diffusive fractionation has a great effect on δ_E modeled from CG (Braud et al., 2009a). Cappa et al. (2003) provided significantly revised diffusivities of water isotopologues (D/D_i in Eq. [7]; Table 2) based on gas kinetic theory as well as experimental results and emphasized the use of skin temperature rather than bulk temperature for fractionation calculations; however, evidence for surface cooling during evaporation from natural water bodies is not yet available. Thus, the diffusivities of Merlivat (1978) are still generally preferred (Lee et al., 2007). Recent evaluations and experimental results from Luz et al. (2009) have also suggested that the Merlivat (1978) values are still valid. If an evaporating body is not well mixed, however, lower temperatures apparently do develop in the top 0.5 mm, and if this temperature structure persists, Cappa et al. (2003) clearly showed that diffusivities and associated kinetic fractionation factors can be quite different from those calculated based on the temperature of the bulk water. This enhanced fractionation may be counteracted by the accumulation of enriched isotopologues at the surface, given the lack of mixing required for significant surface cooling to occur (Horita et al., 2008).

Modeling the Isotopic Composition of Soil Water Vapor and Soil Evaporation

Due to the difficulty in soil water vapor isotope (δ_V) sampling in the past, there is little information on δ_V directly collected from soil profiles (Mathieu and Bariac, 1996). Direct measurements of in situ soil water vapor δ_V are now possible and will provide a direct check for the utilization of the CG model under various conditions, especially for dry soils. An important missing component in the application of the CG model to soil evaporation is the effect of the water potential on the activity of water, which can be easily incorporated with measurements of soil moisture or soil water potential, as developed below.

In recent years, transport-based isotope models such as SiSPAT-Isotope (Braud et al., 2005a, 2009a) and Soil-Litter-Iso (Haverd and Cuntz, 2010; Haverd et al., 2011) have been developed to model soil δ_E, building from analytical solutions for idealized cases that were developed previously (Barnes and Allison, 1983). The Soil-Litter-Iso model was compared with other analytical frameworks (Haverd and Cuntz, 2010), and recent testing of the model against water vapor isotopic composition data from a chamber placed on top of the soil yielded very promising results. The model captured diurnal patterns and a 10-d dry-down quite well, although a mean deviation of around 10‰ was observed for δ^2H between measured and modeled values (Haverd et al., 2011). The SiSPAT-Isotope model was tested using a laboratory column setup, and parameters were calibrated to maximize the model–data agreements. The results indicate that the evaporative enrichment process is very sensitive to changes in kinetic fractionation (Braud et al., 2009a).

The numerical models have introduced many important soil parameters, such as soil moisture, tortuosity, and water potential, which are not explicitly considered in the CG modeling framework. The effect of these parameters could be lumped into the kinetic isotope fractionation factor (α_k) to improve the agreement between model output and observational data for each time step and soil layer in the model. The missing key component to test these effects is the direct measurement of δ_E and authentic δ_V measurements. The mass-balance framework developed by Wang et al. (2012) for direct and continuous quantification of the isotopic composition of leaf transpiration could be adopted for quantifying soil δ_E from measurements, which then can be verified using authentic in situ soil water vapor δ_V measurements.

The surface boundary condition of the most recent bare soil evaporation numerical model provides an isotope evaporative flux based on equilibrium (α_e) and kinetic fractionation (α_k) factors, as well as heat and moisture conservation equations solved for the soil–air interface (Haverd and Cuntz, 2010). The α_k calculation involves adjusting the molecular diffusivity ratio of isotopologues by the aerodynamic parameter n, analogous to Eq. [5]:

$$\alpha_{k,L/V} = \left(\frac{D_i}{D}\right)^n \quad [7]$$

This equation has taken on various forms in models, as summarized and evaluated by Braud et al. (2005b). In an attempt to incorporate the laminar flow development of the soil as it dries, n is related to the volumetric soil moisture (θ) as first proposed by Mathieu and Bariac (1996) and adopted in subsequent numerical models (Braud et al., 2005b, 2009a; Haverd and Cuntz, 2010). This relationship allows n to vary between 0.5 for saturated conditions and 1 for dry soil ("residual" soil moisture) where the laminar layer will have fully developed:

$$n = \frac{(\theta_0 - \theta_r)n_a + (\theta_s - \theta_0)n_s}{\theta_s - \theta_r} \quad [8]$$

where $n_a = 0.5$ and $n_s = 1$, and subscripts s, r, and 0 refer to saturated, residual, and ambient soil moisture content at the evaporating surface, respectively. In the original formulation, θ_r was defined as the minimum soil moisture reached when the soil is in equilibrium with the atmosphere (Mathieu and Bariac, 1996).

The numerical models also include the humidity of the soil modeled from the soil water potential as part of their evaporative flux formulation (Braud et al., 2005a, 2009a; Mathieu and Bariac, 1996); however, they do not take into account the relationship between the water potential and the activity of the water, a_w, which is provided by the Kelvin equation (Barnes and Gentle, 2011; Gee et al., 1992):

$$\ln(a_w) = \frac{\psi_0 M_w}{R T_0 \rho_w} \quad [9]$$

where ψ_0 is soil water potential (kPa) of the evaporating surface, M_w is the molecular weight of water (18.0148 g mol^{-1}), R is the ideal gas constant (8.3145 mL MPa mol^{-1} K^{-1}), ρ_w is the density of water, and T_0 is the temperature (K) of the evaporating surface.

The activity of water is equivalent to the relative humidity in the soil under liquid–vapor equilibrium, a relationship that is commonly used to measure the water potential in soils through devices that measure the dew point in a sealed chamber that contains a soil sample (Gee et al., 1992). When considered with the CG model framework, a reduction in a_w increases the normalized humidity h_A' (Eq. [6]), reducing $\varepsilon_{k,L/V}$ (Eq. [5]), and ultimately affecting the δ_E calculation (Eq. [4]). This modification of h_A' is identical to normalization using the activity of water in saline waters (Horita et al., 2008). Thus, it can be easily incorporated into CG formulations by combining Eq. [6] and [9]. The effect of including the water potential in a CG model calculation of δ_E is illustrated with measurements of a soil profile at Mpala Research Center, Kenya in the case study below.

In addition to the effects of the water potential on fractionation during evaporation, the relationship between equilibrium fractionation in soils and the water potential has yet to be rigorously described. There are strong indications from the equilibration of CO_2 with soil water that dry soils exhibit a different equilibrium behavior than wet soils (Hsieh et al., 1998; Wassenaar et al., 2008). In reviewing some field collections of soil water vapor, Mathieu and Bariac (1996) commented that in dry soils the observed vapor was more enriched than would be expected from equilibrium fractionation at the given temperature. Changes in water structure and properties such as vapor pressure due to confinement in small spaces such as soil pores have been recently reported for bulk water in C nanotubes (Chaplin, 2010) and for H isotopes in water adsorbed to porous silica tubes, leading to significant differences in equilibrium isotope fractionation between the liquid and vapor phases (Richard et al., 2007).

An interesting early experiment on water isotopic fractionation in clays (Stewart, 1972) used a saturated KCl solution as the moisture source for vapor that was allowed to equilibrate with a thin layer of dried clay. In this KCl vapor–clay system, a wide range of isotopic fractionation factors was observed [$\alpha_{L/V}(^2H)_{clay} = 0.93$–$1.06$, with a median of 1.04; HDO concentration ratios of Stewart (1972) were divided by the estimated $\alpha_{L/V}(^2H)_{KCl} = 1.06$]. The temperatures weren't controlled, and a value of $\alpha_{L/V}(^2H)_{KCl}$ as low as 1.06 would require a temperature >40°C using Eq. [3] (Horita and Wesolowski, 1994). Nevertheless, the indication is that $\alpha_{L/V}(^2H)_{clay}$ can have a wide range but with values below the isotopic fractionation factor for free water at a given temperature. Interestingly, the recent analogous work with porous silica tubes instead of clays (Richard et al., 2007) found $\alpha_{L/V}(^2H)$ values of around 1.03 at 20% relative humidity and 1.05 at 80% relative humidity at around 20°C, compared with 1.085 from Eq. [3]. Thus, these results are somewhat consistent with the less-controlled early study with clays, suggesting that the equilibrium isotopic fractionation between vapor and water adsorbed on clays is lower than the free water value at the same temperature.

A final consideration toward understanding the isotopic composition of soil water vapor is the organization of water molecules within the liquid phase. It has been shown that enriched isotopologues exist at higher concentrations near dissolved ions and thus near particle surfaces (Phillips and Bentley, 1987). Given this structure, there could potentially be a concentration of depleted isotopes near the evaporating surface of pore water. This "hydration sphere isotope effect" would cause isotopic differences between the bulk water and the evaporating surface and require a stagnant solution, similar to the skin temperature effect shown by Cappa et al. (2003). The impact of isotopic gradients within individual pockets of liquid soil water on δ_E has not been explored. If an isotopic difference exists between the bulk water and the evaporating surface, this could be another reason to use equilibration analytical methods on undisturbed soils for estimating the liquid isotopic composition (Herbstritt et al., 2012; Hsieh et al., 1998; Scrimgeour, 1995; Wassenaar et al., 2008).

The isotopic composition of soil evaporation is the result of several different fractionation processes. First, the phase change

and equilibrium processes within the soil matrix are governed by temperature and the soil water potential. Kinetic fractionation is affected by the physical characteristics of the diffusion path (e.g., tortuosity) as well as isotopic gradients between the site of evaporation and the initiation of turbulent mixing just above the soil surface. Vapor moving vertically through the soil will also probably re-equilibrate with the liquid water along its path. The overall apparent fractionation between liquid water at any given depth and the resultant evaporative flux leaving the soil surface reflects all of these fractionation processes. As the liquid water sources for soil evaporation fluctuate in depth and isotopic composition, modeling the soil evaporation isotopic end member accurately at any given time becomes very difficult. Thus, techniques for measuring the evaporated vapor itself will be very important as this field moves forward.

Case Study: Soil Water Vapor in an African Savanna

An example of direct soil water vapor isotope measurement is shown in Fig. 1, with data from a single profile collected at Mpala Research Centre, Kenya, on 29 Mar. 2011 from 12:45 to 13:00 h. The soil is a red sandy loam with a bulk density of 1.45 g cm^{-3} and a porosity of 0.45. The vegetation is mixed semiarid savanna, and the local mean annual precipitation is around 600 mm. Soil vapor was sampled at four depths (5, 10, 20, and 30 cm; sampled in depth order starting with 5 cm) via buried Teflon tubing, with the final 10 cm of each tube perforated and packed with glass wool. Soil vapor was drawn directly into a laser water vapor isotope analyzer (DLT100, Los Gatos Research) at a flow rate of 150 to 180 mL min^{-1}, diluted with ambient air (intake at 2 m above ground) for a total flow of 400 mL min^{-1}. This dilution allowed reduced flow rates at the soil vapor intakes and lowered the humidity in the tubing and analytical equipment to reduce the chance of condensation forming. Data were collected for around 90 s at each depth. The soil temperature was measured with Campbell Scientific TCAV averaging soil temperature probes at 5 and 20 cm, and a linear profile was assumed for 10 and 30 cm. The ambient atmospheric water vapor isotopic composition, humidity, and temperature were sampled at 2 m above the ground surface. Soil samples were collected from an auger hole adjacent to the buried tubing immediately after vapor sampling. The water potential was measured via a Decagon Devices WP4T dew point potentiometer. Liquid soil water was isolated via cryogenic vacuum distillation (West et al., 2006) and analyzed with a continuous-flow water vapor isotope analyzer using a heated nebulizer for sample introduction (WVISS, Los Gatos Research).

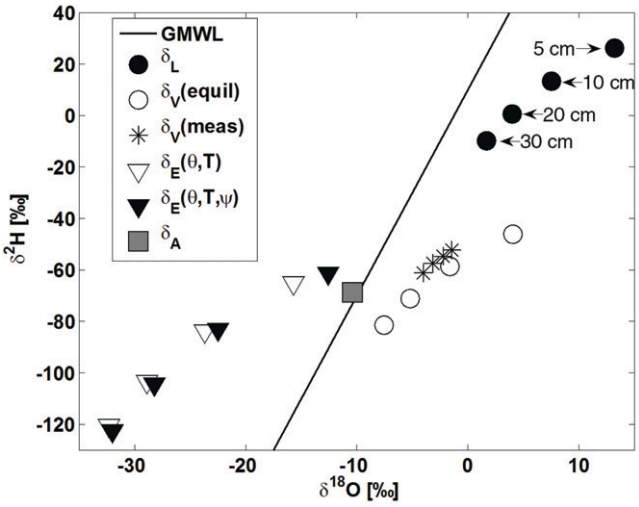

Fig. 1. Measured and calculated isotope values of liquid- (δ_L) and vapor-phase (δ_V) water from a soil profile sampled 29 Mar. 2011 in a sandy loam soil at the Mpala Research Center, Kenya (see Table 3). Sampling depths are shown for the liquid soil water samples, and each set of vapor values follows the same depth sequence. Two sets of δ_V values are shown: δ_V(meas) was measured directly in the field with a water vapor isotope analyzer (DLT-100, Los Gatos Research Inc.); δ_V(equil) was calculated using soil temperature and liquid soil water isotopic composition (Eq. [1–3]). Craig–Gordon model isotope values of the evaporate (δ_E) were calculated in two ways: $\delta_E(\theta,T)$ was calculated conventionally, considering volumetric water content θ and soil temperature T (Eq. [2–8]); $\delta_E(\theta,T,\psi)$ was calculated by additionally considering soil water potential ψ (Eq. [2–9]). Also shown is the isotopic ratio of the atmosphere (δ_A); GMWL is the global meteoric water line.

Equilibrium water vapor isotopic compositions were calculated for each depth based on the respective measured liquid soil water isotopic composition, soil temperature, and the associated fractionation factors (Eq. [1–3]). For each depth, the corresponding CG modeled values were calculated in two ways: (i) conventionally, using Eq. [2–8] assuming $a_w = 1$ [Fig. 1; Table 3; $\delta_E(\theta,T)$]; and (ii) including the soil water potential by calculating a_w with Eq. [9] [$\delta_E(\theta,T,\psi)$]. The parameters for CG calculations are given in Table 3 with specific examples and typical ranges.

The measured soil vapor isotope values fell close to those that would be expected for isotopic equilibrium at the temperature for each depth (Fig. 1). The measured values cover a reduced range (−4.0 to −2.2‰ for δ^{18}O) relative to the equilibrium values (−7.5 to 4.1‰ for δ^{18}O), but have similar mean values of −2.8 and −3.0‰ for δ^{18}O and −57 and −65‰ for δ^2H, respectively. These mean values are weighted by soil moisture contents (θ_0) of 5.3, 6.0, 6.2, and 6.6% (v/v) for the 5-, 10-, 20-, and 30-cm depths, respectively. The fact that the measured vapor isotope values fall in a smaller range, but within the calculated equilibrium values, suggests that either the sampling process induced mixing of vapor from various depths or that the vapor is somewhat mixed within the sampling depths at this time of day. Sampling-induced mixing is likely given that around 0.5 to 0.6 L of soil was influenced by the sampling at each depth. Subtracting the volumetric water contents from a porosity of 0.45 gives air-filled porosity values of 0.38 to 0.39, resulting in a radius of influence of about 7 cm around each perforated section of tubing, suggesting that the sampling depths overlapped to some degree. The three sets of values—liquid, measured vapor, and equilibrium vapor—have similar slopes of 3.1, 3.4, and 3.0 (δ^2H vs. δ^{18}O). Although this

level of consistency among slopes is encouraging within the scope of this study, a second study is needed to examine the differences in these slopes relative to differences in fractionation factors as well as the combined uncertainties in δ^2H and $\delta^{18}O$. Interestingly, the measured soil water vapor isotope values are much closer to the equilibrium vapor isotope values than the CG-modeled δ_E values (Fig. 1). This example is therefore consistent with the typical assumption of isotopic equilibrium between liquid and vapor in the soil (e.g., Mathieu and Bariac, 1996).

The effect of including water activity (i.e., the soil water potential, ψ) in the CG calculations depends on the relationships among equilibrium vapor, ambient vapor, and ambient humidity. To examine these relationships as well as the effect of including soil water content (θ), we made a series of CG calculations starting with the 5-cm-depth parameters of Fig. 1 and Table 3. We varied ψ_0 and calculated θ_0 using a relationship of the form

$$\theta = \left(\frac{a}{-\psi}\right)^{1/b} \qquad [10]$$

where $a = 0.00109$ and $b = 3.46$ based on 410 paired measurements of ψ and θ for 14 separate drying experiments. The measured values ranged from −0.2 to −61 MPa for ψ and 1 to 41% (v/v) for θ.

We then calculated δ_E using Eq. [2–9] (Fig. 2, solid black lines). We also varied three atmospheric parameters: T_A, the isotopic ratio of the atmosphere δ_A, and h_A (Fig. 2, dashed black lines). Lastly, we made the same calculations without considering θ (i.e., $n = 1$) or ψ (i.e., $a_w = 1$), and used both conventional (Merlivat, 1978) and revised (Cappa et al., 2003) values for equilibrium isotope fractionation factors (Fig. 2, gray lines). From these calculations it is clear that for drying soils, the effect of including ψ can be similar to or greater than the effect of including θ (i.e., changing n from 0.5 to 1). Including θ (Eq. [8]), which leads to $n = 0.5$ in the wettest soils (θ_0 close to 0 MPa), leads to more enriched δ_E values in wetter soils. Including ψ (Eq. [9]) apparently leads to the opposite effect, with more enriched δ_E values in drier soils. Both mechanisms can be correct, with the former (lower n and higher δ_E in wetter soils) describing the decrease in kinetic fractionation as the soil evaporation becomes more controlled by atmospheric turbulence than by diffusion in the soil (Mathieu and Bariac, 1996). The latter (higher h_A' and higher δ_E in drier soils) simply describes the effect of lower water activity on the saturation vapor pressure in the soil. This soil water potential effect can also be as large as the impact of using the drastically different diffusivity ratios of Cappa et al. (2003) rather than those of Merlivat (1978).

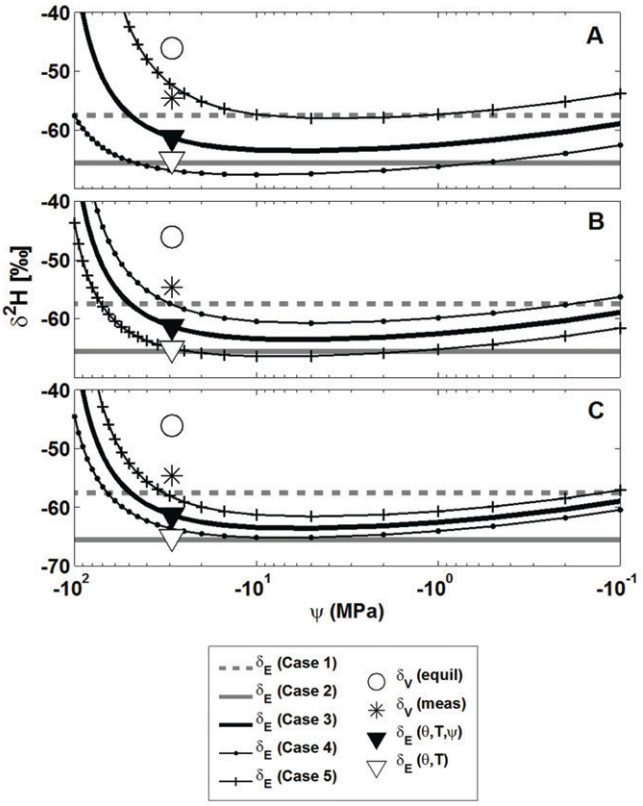

Fig. 2. Craig–Gordon (CG) model calculations for δ^2H across a range of soil water potentials (ψ) and ambient atmospheric parameters. The CG soil evaporate (δ_E) was calculated using Eq. [2–9]. The measured [δ_V(meas)] and calculated [δ_V(equil)] correspond to the 5-cm-depth example of Table 3 and Fig. 1. Each panel shows five cases. Cases 1 and 2 were calculated without considering soil moisture content (θ) or soil water potential (ψ; i.e., soil pore space saturation parameter $n = 1$ and activity of water $a_w = 1$), and use the contrasting kinetic isotope fractionation factor α_k values of Cappa et al. (2003) and Merlivat (1978), respectively. Cases 3, 4, and 5 show the effects of varying one of three atmospheric parameters: (A) relative humidity (h_A), (B) water vapor isotopic composition (δ_A), and (C) temperature (T_A). Case 3 always used the measured values ($h_A = 0.331$, $\delta_A = -68.7$‰, $T_A = 28.8$°C), whereas Cases 4 and 5 used lower and higher bounds, respectively, of a range that could be expected in the field ($h_A \pm 0.1$, $\delta_A \pm 5$‰, and $T_A \pm 2$°C).

Conclusions

We have summarized all the available modeling and field methods to quantify the isotopic composition of water vapor, with a focus on the soil–plant–atmosphere continuum. When applying the CG modeling framework to soil evaporation, we suggest the inclusion of the soil water potential in the normalization of "free atmosphere" humidity to the evaporating surface (Eq. [6] and [9]), just as water activity is included in the normalization for evaporation from saline waters. This will reduce the total fractionation for evaporation from unsaturated soils as predicted by the CG model. Such a reduction is consistent with observations of enriched soil water vapor and can be significant in soils with water potentials drier than around −10 MPa. This improvement is easily implemented in all CG formulations, and the only additional measurement required is the soil water potential. This parameter can also be calculated from the soil water content using an appropriate soil water retention curve. There is also a possibility that leaf water potential could be used to improve the use of normalized humidity in application of the CG model to evaporative isotopic enrichment in leaves (e.g., Cuntz et al., 2007), although the

leaf water potential is highly variable and more difficult to estimate than the soil water potential.

Another feature of isotopic fractionation in soil water that is likely to change through experimentation is the equilibrium fractionation factor. The equilibrium fractionation for free water is still represented empirically. The indication from experiments between vapor and water adsorbed onto clay and silica tubes is that liquid–vapor equilibrium fractionation is substantially reduced in a porous medium setting relative to free water. The structure of water changes in confined spaces, and it is expected that the nature of pore spaces in different types of soils will lead to different equilibrium fractionation factors. The use of stable isotopes of water vapor in understanding the soil–plant–atmosphere continuum at various scales depends on an accurate understanding of fractionation processes and the associated modeling of isotopic fluxes in the environment. The relatively new analytical capabilities for water vapor isotopes coupled with novel sampling approaches under development will provide the necessary data to follow these fractionation processes in situ.

Appendix: Definitions

The isotope nomenclature used here is consistent with the most recent guidelines (Coplen, 2011) where the decimal values are used in all calculations and per-mil (‰) values are for display purposes only. We use the term *vapor* to refer to water vapor only, and other gaseous constituents are referred to as *gas*. We are explicit about the direction of the isotopic fractionation factors (e.g., $\alpha_{L/V} = R_L/R_V = \varepsilon_{L/V} + 1$), and where no isotope is specified, α can refer to either O or H fractionation.

a_w thermodynamic activity of water
D diffusion coefficient, with subscript i indicating the minor isotopologue, $m^2\ s^{-1}$
e_{s0} saturation vapor pressure at the evaporating surface, kPa
e_{sA} saturation vapor pressure in the atmosphere, kPa
h_0 humidity of the evaporating surface
h_A humidity of the atmosphere; h_A' is normalized to the evaporating surface
n aerodynamic parameter for adjusting diffusivity ratios
${}^iR_p$ isotope ratio of minor isotopologue i to the abundant isotopologue in phase p
R ideal gas constant, L kPa $mol^{-1}\ K^{-1}$, distinguished from the isotope ratio (e.g., ${}^{18}R_L$) by having no superscripts or subscripts
T_0 temperature of the evaporating surface, K
T_A temperature of the atmosphere, K
α_e kinetic isotopic fractionation factor
α_k equilibrium isotopic fractionation factor
δ_A relative difference of isotope ratios of the atmosphere
δ_E relative difference of isotope ratios of the evaporate
δ_L relative difference of isotope ratios of soil liquid
δ_V relative difference of isotope ratios of soil vapor
ε_k kinetic isotopic fractionation ($\varepsilon_k = \alpha_k - 1$)
θ_0 volumetric water content of the evaporating surface, $m^3\ m^{-3}$
θ_s saturated volumetric water contents, $m^3\ m^{-3}$
θ_r residual volumetric water contents, $m^3\ m^{-3}$
ρ_w density of water, $kg\ m^{-3}$
ψ_0 water potential at the evaporating surface, MPa

Acknowledgments

This project was funded by the National Science Foundation through a CAREER award to K.K. Caylor (EAR847368); L. Wang also acknowledges the financial support from a vice-chancellor's postdoctoral research fellowship at the University of New South Wales. We greatly appreciate the field and laboratory assistance of Ekomwa Akuwam, John Maina Gitonga, and the staff at Mpala Research Centre.

References

Abramova, M.M. 1969. Movement of moisture as liquid and vapor in soils of semi-deserts. In: P.E. Rytema and H. Wassink, editors, Wageningen symposium on water in the unsaturated zone. IASH-UNESCO, Gentbrugge, Belgium. p. 781–789.

Allison, G.B., and C.J. Barnes. 1983. Estimation of evaporation from non-vegetated surfaces using natural deuterium. Nature 301:143–145. doi:10.1038/301143a0

Araguás-Araguás, L., K. Froehlich, and K. Rozanski. 2000. Deuterium and oxygen-18 isotope composition of precipitation and atmospheric moisture. Hydrol. Processes 14:1341–1355. doi:10.1002/1099-1085(20000615)14:83.0.CO;2-Z

Araguás-Araguás, L., K. Rozanski, R. Gonfiantini, and D. Louvat. 1995. Isotope effects accompanying vacuum extraction of soil-water for stable-isotope analyses. J. Hydrol. 168:159–171. doi:10.1016/0022-1694(94)02636-P

Barnes, C.J., and G.B. Allison. 1983. The distribution of deuterium and 18O in dry soils: 1. Theory. J. Hydrol. 60:141–156. doi:10.1016/0022-1694(83)90018-5

Barnes, C.J., and G.B. Allison. 1988. Tracing of water movement in the unsaturated zone using stable isotopes of hydrogen and oxygen. J. Hydrol. 100:143–176. doi:10.1016/0022-1694(88)90184-9

Barnes, G., and I. Gentle. 2011. Introduction to interfacial science. Oxford Univ. Press, Oxford, UK.

Bittelli, M., F. Ventura, G.S. Campbell, R.L. Snyder, F. Gallegati, and P.R. Pisa. 2008. Coupling of heat, water vapor, and liquid water fluxes to compute evaporation in bare soils. J. Hydrol. 362:191–205. doi:10.1016/j.jhydrol.2008.08.014

Braud, I., T. Bariac, P. Biron, and M. Vauclin. 2009a. Isotopic composition of bare soil evaporated water vapo: II. Modeling of RUBIC IV experimental results. J. Hydrol. 369:17–29. doi:10.1016/j.jhydrol.2009.01.038

Braud, I., T. Bariac, J.-P. Gaudet, and M. Vauclin. 2005a. SiSPAT-Isotope, a coupled heat, water and stable isotope (HDO and $H_2{}^{18}O$) transport model for bare soil: I. Model description and first verifications. J. Hydrol. 309:277–300. doi:10.1016/j.jhydrol.2004.12.013

Braud, I., T. Bariac, M. Vauclin, Z. Boujamlaoui, J.-P. Gaudet, P. Biron, and P. Richard. 2005b. SiSPAT-Isotope, a coupled heat, water and stable isotope (HDO and $H_2{}^{18}O$) transport model for bare soil: II. Evaluation and sensitivity tests using two laboratory data sets. J. Hydrol. 309:301–320. doi:10.1016/j.jhydrol.2004.12.012

Braud, I., P. Biron, T. Bariac, P. Richard, L. Canale, J.P. Gaudet, and M. Vauclin. 2009b. Isotopic composition of bare soil evaporated water vapor: I. RUBIC IV experimental setup and results. J. Hydrol. 369:1–16. doi:10.1016/j.jhydrol.2009.01.034

Brooks, J.R., H.R. Barnard, R. Coulombe, and J.J. McDonnell. 2010. Ecohydrologic separation of water between trees and streams in a Mediterranean climate. Nat. Geosci. 3:100–104. doi:10.1038/ngeo722

Brunel, J.P., H.J. Simpson, A.L. Herczeg, R. Whitehead, and G.R. Walker. 1992. Stable isotope composition of water vapor as an indicator of transpiration fluxes from rice crops. Water Resour. Res. 28:1407–1416. doi:10.1029/91WR03148

Campbell, G.S., and J.M. Norman. 1998. An introduction to environmental biophysics. Springer, New York.

Cane, G., and I.D. Clark. 1999. Tracing ground water recharge in an agricultural watershed with isotopes. Ground Water 37:133–139. doi:10.1111/j.1745-6584.1999.tb00966.x

Cappa, C.D., M.B. Hendricks, D.J. DePaolo, and R.C. Cohen. 2003. Isotopic fractionation of water during evaporation. J. Geophys. Res. 108:4525. doi:10.1029/2003JD003597

Chaplin, M.F. 2010. Structuring and behavior of water in nanochannels and confined spaces. In: L.J. Dunne and G. Manos, editors, Adsorption and phase behavior in nanochannels and nanotubes. Springer, New York. p. 241–255.

Chialvo, A.A., and J. Horita. 2009. Liquid–vapor equilibrium isotopic fractionation of water: How well can classical water models predict it? J. Chem. Phys. 130:094509. doi:10.1063/1.3082401

Coplen, T.B. 2011. Guidelines and recommended terms for expression of stable isotope-ratio and gas-ratio measurement results. Rapid Commun. Mass Spectrom. 25:2538–2560.

Craig, H. 1961. Isotopic variations in meteoric waters. Science 133:1702–1703. doi:10.1126/science.133.3465.1702

Craig, H., and L.I. Gordon. 1965. Deuterium and oxygen-18 variations in the ocean and marine atmosphere. In: E. Tongiorgi, editor, Stable isotopes in oceanographic studies and paleotemperatures, Proceedings, Spoleto, Italy. Consiglio Nazionale delle Ricerche, Lab. de Geologia Nucleare, Pisa, Italy. p. 9–130.

Cuntz, M., J. Ogée, G. Farquhar, P. Peylin, and L.A. Cernusak. 2007. Modelling advection and diffusion of water isotopologues in leaves. Plant Cell Environ. 30:892–909. doi:10.1111/j.1365-3040.2007.01676.x

Dansgaard, W. 1953. The abundance of ^{18}O in atmospheric water and water vapor. Tellus 5:461–469. doi:10.1111/j.2153-3490.1953.tb01076.x

Dawson, T.E. 1993. Hydraulic lift and water use by plants: Implications for water balance, performance and plant–plant interactions. Oecologia 95:565–574. doi:10.1007/BF00317442

Dawson, T.E. 1996. Determining water use by trees and forests from isotopic, energy balance and transpiration analyses: The roles of tree size and hydraulic lift. Tree Physiol. 16:263–272. doi:10.1093/treephys/16.1-2.263

Dawson, T.E., S. Mambelli, A.H. Plamboeck, P.H. Templer, and K.P. Tu. 2002. Stable isotopes in plant ecology. Annu. Rev. Ecol. Syst. 33:507–559. doi:10.1146/annurev.ecolsys.33.020602.095451

de Groot, P.A. 2009. Handbook of stable isotope analytical techniques. Vol. 2. Elsevier, New York.

de Laeter, J.R., J.K. Böhlke, P. De Bièvre, H. Hidaka, H.S. Peiser, K.J.R. Rosman, and P.D.P. Taylor. 2003. Atomic weights of the elements: Review 2000. Pure Appl. Chem. 75:683–800. doi:10.1351/pac200375060683

D'Odorico, P., K. Caylor, G.S. Okin, and T.M. Scanlon. 2007. On soil moisture–vegetation feedbacks and their possible effects on the dynamics of dryland ecosystems. J. Geophys. Res. 112:G04010. doi:10.1029/2006JG000379

Ehleringer, J.R., and T.E. Dawson. 1992. Water uptake by plants: Perspectives from stable isotope composition. Plant Cell Environ. 15:1073–1082. doi:10.1111/j.1365-3040.1992.tb01657.x

Ehleringer, J.R., S. Schwinning, and R. Gebauer. 1999. Water use in arid land ecosystems. In: M.C. Press, editor, Advances in plant physiological ecology. Blackwell Science, Oxford, UK. p. 347–365.

Ellsworth, P.Z., and D.G. Williams. 2007. Hydrogen isotope fractionation during water uptake by woody xerophytes. Plant Soil 291:93–107. doi:10.1007/s11104-006-9177-1

Feddes, R.A., H. Hoff, M. Bruen, T. Dawson, P. de Rosnay, P. Dirmeyer, et al. 2001. Modeling root water uptake in hydrological and climate models. Bull. Am. Meteorol. Soc. 82:2797–2809. doi:10.1175/1520-0477(2001)0822.3.CO;2

Flanagan, L.B., and J.R. Ehleringer. 1991. Stable isotope composition of stem and leaf water: Applications to the study of plant water use. Funct. Ecol. 5:270–277. doi:10.2307/2389264

Gat, J.R. 1996. Oxygen and hydrogen isotopes in the hydrologic cycle. Annu. Rev. Earth Planet. Sci. 24:225–262. doi:10.1146/annurev.earth.24.1.225

Gee, G.W., M.D. Campbell, G.S. Campbell, and J.H. Campbell. 1992. Rapid measurement of low soil-water potential using a water activity meter. Soil Sci. Soc. Am. J. 56:1068–1070. doi:10.2136/sssaj1992.03615995005600040010x

Gonfiantini, R. 1978. Standards for stable isotope measurements in natural compounds. Nature 271:534–536. doi:10.1038/271534a0

Good, S., K. Soderberg, L. Wang, and K. Caylor. 2012. Uncertainties in the assessment of the isotopic compositionof surface fluxes: A direct comparison of techniques using laser-based water vapor isotope analyzers. J. Geophys. Res. Atmos. doi:10.1029/2011JD017168

Griffis, T., J. Baker, S. Sargent, B. Tanner, and J. Zhang. 2004. Measuring field-scale isotopic CO2 fluxes with tunable diode laser absorption spectroscopy and micrometeorological techniques. Agric. For. Meteorol. 124:15–29. doi:10.1016/j.agrformet.2004.01.009

Griffis, T.J., S.D. Sargent, X. Lee, J.M. Baker, J. Greene, M. Erickson, et al. 2010. Determining the oxygen isotope composition of evapotranspiration using eddy covariance. Boundary-Layer Meteorol. 137:307–326. doi:10.1007/s10546-010-9529-5

Han, L.-F., M. Groening, P. Aggarwal, and B.R. Helliker. 2006. Reliable determination of oxygen and hydrogen isotope ratios in atmospheric water vapour adsorbed on 3A molecular sieve. Rapid Commun. Mass Spectrom. 20:3612–3618. doi:10.1002/rcm.2772

Hanisco, T.F., E.J. Moyer, E.M. Weinstock, J.M. St. Clair, D.S. Sayres, J.B. Smith, et al. 2007. Observations of deep convective influence on stratospheric water vapor and its isotopic composition. Geophys. Res. Lett. 34:L04814. doi:10.1029/2006GL027899

Harmathy, T.Z. 1969. Simultaneous moisture and heat transfer in porous systems with particular reference to drying. Res. Pap. 407. Natl. Res. Counc. Canada, Ottawa, ON.

Haverd, V., and M. Cuntz. 2010. Soil–Litter–Iso: A one-dimensional model for coupled transport of heat, water and stable isotopes in soil with a litter layer and root extraction. J. Hydrol. 388:438–455. doi:10.1016/j.jhydrol.2010.05.029

Haverd, V., M. Cuntz, D. Griffith, C. Keitel, C. Tadros, and J. Twining. 2011. Measured deuterium in water vapour concentration does not improve the constraint on the partitioning of evapotranspiration in a tall forest canopy, as estimated using a soil vegetation atmosphere transfer model. Agric. For. Meteorol. 151:645–654. doi:10.1016/j.agrformet.2011.02.005

Helliker, B.R., and S.L. Richter. 2008. Subtropical to boreal convergence of tree-leaf temperatures. Nature 454:511–514. doi:10.1038/nature07031

Helliker, B.R., J.S. Roden, C. Cook, and J.R. Ehleringer. 2002. A rapid and precise method for sampling and determining the oxygen isotope ratio of atmospheric water vapor. Rapid Commun. Mass Spectrom. 16:929–932 10.1002/rcm.659. doi:10.1002/rcm.659

Henschel, J.R., and M.K. Seely. 2008. Ecophysiology of atmospheric moisture in the Namib Desert. Atmos. Res. 87:362–368. doi:10.1016/j.atmosres.2007.11.015

Herbstritt, B., B. Gralher, and M. Weiler. 2012. Continuous in situ measurements of stable isotopes in liquid water. Water Resour. Res. 48:W03601. doi:10.1029/2011WR011369

Hesterberg, R., and U. Siegenthaler. 1991. Production and stable isotopic composition of CO2 in a soil near Bern, Switzerland. Tellus B 43:197–205.

Hoffmann, G., J. Jouzel, and V. Masson. 2000. Stable water isotopes in atmospheric general circulation models. Hydrol. Processes 14:1385–1406. doi:10.1002/1099-1085(20000615)14:83.0.CO;2-1

Horita, J. 2005. Saline waters. In: P.K. Aggarwal et al., editors, Isotopes in the water cycle: Past, present and future of a developing science. Springer, Dordrecht, the Netherlands. p. 271–287.

Horita, J., K. Rozanski, and S. Cohen. 2008. Isotope effects in the evaporation of water: A status report of the Craig–Gordon model. Isot. Environ. Health Stud. 44:23–49. doi:10.1080/10256010801887174

Horita, J., and D.J. Wesolowski. 1994. Liquid–vapor fractionation of oxygen and hydrogen isotopes of water from the freezing to the critical temperature. Geochim. Cosmochim. Acta 58:3425–3437. doi:10.1016/0016-7037(94)90096-5

Hsieh, J.C.C., S.M. Savin, E.F. Kelly, and O.A. Chadwick. 1998. Measurement of soil-water $\delta^{18}O$ values by direct equilibration with CO2. Geoderma 82:255–268. doi:10.1016/S0016-7061(97)00104-3

Humphries, S.D., S.M. Clegg, T. Rahn, J.E. Fessenden, L. Dobeck, L. Spangler, and T.L. McLing. 2010. Measurements of CO_2 carbon stable isotopes at artificial and natural analog sites. Paper presented at: American Geophysical Union Fall Meeting, San Francisco. 13–17 Dec. 2010. Abstract U21A-0008.

Jackson, R., L. Moore, W. Hoffman, W. Pockman, and C. Linder. 1999. Ecosystem rooting depth determined with caves and DNA. Proc. Natl. Acad. Sci. 96:11387–11392. doi:10.1073/pnas.96.20.11387

Jacob, H., and C. Sonntag. 1991. An 8-year record of the seasonal variation of ^{2}H and ^{18}O in atmospheric water vapor and precipitation at Heidelberg, Germany. Tellus B 43:291–300. doi:10.1034/j.1600-0889.1991.t01-2-00003.x

Japas, M.L., R. Fernandez-Prini, J. Horita, and D.J. Wesolowski. 1995. Fractioning of isotopic species between coexisting liquid and vapor water: Complete temperature range, including the asymptotic critical behavior. J. Phys. Chem. 99:5171–5175. doi:10.1021/j100014a043

Jouzel, J., and R.D. Koster. 1996. A reconsideration of the initial conditions used for stable water isotope models. J. Geophys. Res. 101(D17):22933–22938. doi:10.1029/96JD02362

Keeling, C.D. 1958. The concentration and isotopic abundances of atmospheric carbon dioxide in rural areas. Geochim. Cosmochim. Acta 13:322–324. doi:10.1016/0016-7037(58)90033-4

Kelly, S.F., and J.S. Selker. 2001. Osmotically driven water vapor transport in unsaturated soils. Soil Sci. Soc. Am. J. 65:1634–1641. doi:10.2136/sssaj2001.1634

Kerstel, E.R.T., R. van Trigt, N. Dam, J. Reuss, and H.A.J. Meijer. 1999. Simultaneous determination of the $^{2}H/^{1}H$, $^{17}O/^{16}O$, and $^{18}O/^{16}O$ isotope abundance ratios in water by means of laser spectrometry. Anal. Chem. 71:5297–5303. doi:10.1021/ac990621e

Kim, K., and X. Lee. 2011. Isotopic enrichment of liquid water during evaporation from water surfaces. J. Hydrol. 399:364–375. doi:10.1016/j.jhydrol.2011.01.008

Lee, J.-E., I. Fung, D.J. DePaolo, and C.C. Henning. 2007. Analysis of the global distribution of water isotopes using the NCAR atmospheric general circulation model. J. Geophys. Res. 112:D16306. doi:10.1029/2006JD007657

Lee, X., and W. Massman. 2011. A perspective on thirty years of the Webb, Pearman and Leuning density corrections. Boundary-Layer Meteorol. 139:37–59. doi:10.1007/s10546-010-9575-z

Lee, X., S. Sargent, R. Smith, and B. Tanner. 2005. In situ measurements of the water vapor 18O/16O isotope ratio for atmospheric and ecological applications. J. Atmos. Ocean. Technol. 22:555–565. doi:10.1175/JTECH1719.1

Luz, B., E. Barkan, R. Yam, and A. Shemesh. 2009. Fractionation of oxygen and hydrogen isotopes in evaporating water. Geochim. Cosmochim. Acta 73:6697–6703. doi:10.1016/j.gca.2009.08.008

Majoube, M. 1971. Oxygen-18 and deuterium fractionation between water and steam. J. Chim. Phys. Phys. Chim. Biol. 68:1423–1438.

Mathieu, R., and T. Bariac. 1996. A numerical model for the simulation of stable isotope profiles in drying soils. J. Geophys. Res. 101(D7):12685–12696. doi:10.1029/96JD00223

Melayah, A., L. Bruckler, and T. Bariac. 1996a. Modeling the transport of water stable isotopes in unsaturated sails under natural conditions: 1. Theory. Water Resour. Res. 32:2047–2054. doi:10.1029/96WR00674

Melayah, A., L. Bruckler, and T. Bariac. 1996b. Modeling the transport of water stable isotopes in unsaturated soils under natural conditions: 2. Comparison with field experiments. Water Resour. Res. 32:2055–2065. doi:10.1029/96WR00673

Merlivat, L. 1978. Molecular diffusivities of $H_2{}^{16}O$, $HD^{16}O$, and $H_2{}^{18}O$ in gases. J. Chem. Phys. 69:2864–2871. doi:10.1063/1.436884

Midwood, A.J., B. Thornton, and P. Millard. 2008. Measuring the ^{13}C content of soil-respired CO_2 using a novel open chamber system. Rapid Commun. Mass Spectrom. 22:2073–2081. doi:10.1002/rcm.3588

Mooney, H.A., S.L. Gulmon, P.W. Rundel, and J. Ehleringer. 1980. Further observations on the water relations of Prosopis tamarugo of the northern Atacama desert. Oecologia 44:177–180. doi:10.1007/BF00572676

Nicholson, S. 2000. Land surface processes and Sahel climate. Rev. Geophys. 38:117–139. doi:10.1029/1999RG900014

Ogée, J., P. Peylin, M. Cuntz, T. Bariac, Y. Brunet, P. Berbigier, et al. 2004. Partitioning net ecosystem carbon exchange into net assimilation and respiration with canopy-scale isotopic measurements: An error propagation analysis with $^{13}CO_2$ and $CO^{18}O$ data. Global Biogeochem. Cycles 18:GB2019. doi:10.1029/2003GB002166

Oi, T. 2003. Vapor pressure isotope effects of water studied by molecular orbital calculations. J. Nucl. Sci. Technol. 40:517–523. doi:10.3327/jnst.40.517

Panday, S., and P.S. Huyakorn. 2008. MODFLOW SURFACT: A state-of-the-art use of vadose zone flow and transport equations and numerical techniques for environmental evaluations. Vadose Zone J. 7:610–631. doi:10.2136/vzj2007.0052

Peters, L.I., and D. Yakir. 2010. A rapid method for the sampling of atmospheric water vapour for isotopic analysis. Rapid Commun. Mass Spectrom. 24:103–108. doi:10.1002/rcm.4359

Philip, J.R., and D.A. de Vries. 1957. Moisture movement in porous materials under temperature gradients. Trans. Am. Geophys. Union 38:222–232.

Phillips, F.M., and H.W. Bentley. 1987. Isotopic fractionation during ion filtration: 1. Theory. Geochim. Cosmochim. Acta 51:683–695. doi:10.1016/0016-7037(87)90079-2

Pollock, W., L.E. Heidt, R. Lueb, and D.H. Ehhalt. 1980. Measurement of stratospheric water vapour by cryogenic collection. J. Geophys. Res. 85:5555–5568. doi:10.1029/JC085iC10p05555

Polyakov, V.B., J. Horita, D.R. Cole, and A.A. Chialvo. 2007. Novel corresponding-states principle approach for the equation of state of isotopologues: H218O as an example. J. Phys. Chem. B 111:393–401. doi:10.1021/jp064055k

Richard, T., L. Mercury, M. Massault, and J.L. Michelot. 2007. Experimental study of D/H isotopic fractionation factor of water adsorbed on porous silica tubes. Geochim. Cosmochim. Acta 71:1159–1169. doi:10.1016/j.gca.2006.11.028

Risi, C., S. Bony, F. Vimeux, C. Frankenberg, D. Noone, and J. Worden. 2010a. Understanding the Sahelian water budget through the isotopic composition of water vapor and precipitation. J. Geophys. Res. 115:D24110. doi:10.1029/2010JD014690

Risi, C., S. Bony, F. Vimeux, and J. Jouzel. 2010b. Water-stable isotopes in the LMDZ4 general circulation model: Model evaluation for present-day and past climates and applications to climatic interpretations of tropical isotopic records. J. Geophys. Res. 115:D24123. doi:10.1029/2010JD015242

Rodriguez-Iturbe, I., and A. Porporato. 2004. Ecohydrology of water-controlled ecosystems: Soil moisture and plant dynamics. Cambridge Univ. Press, Cambridge, UK.

Rothfuss, Y., P. Biron, I. Braud, L. Canale, J.-L. Durand, J.-P. Gaudet, et al. 2010. Partitioning evapotranspiration fluxes into soil evaporation and plant transpiration using water stable isotopes under controlled conditions. Hydrol. Processes 24:3177–3194. doi:10.1002/hyp.7743

Rozanski, K. 2005. Isotopes in atmospheric moisture. In: P. K. Aggarwal et al., editors, Isotopes in the water cycle: Past, present and future of a developing science. Springer, Dordrecht, the Netherlands. p. 291–302.

Scanlon, T.M., K.K. Caylor, S. Levin, and I. Rodriguez-Iturbe. 2007. Positive feedbacks promote power-law clustering of Kalahari vegetation. Nature 449:209–213. doi:10.1038/nature06060

Schneider, M., K. Yoshimura, F. Hase, and T. Blumenstock. 2010. The ground-based FTIR network's potential for investigating the atmospheric water cycle. Atmos. Chem. Phys. 10:3427–3442. doi:10.5194/acp-10-3427-2010

Scrimgeour, C.M. 1995. Measurement of plant and soil water isotope composition by direct equilibration methods. J. Hydrol. 172:261–274. doi:10.1016/0022-1694(95)02716-3

Shurbaji, A.-R.M., and F.M. Phillips. 1995. A numerical model for the movement of H2O, H218O, and 2HHO in the unsaturated zone. J. Hydrol. 171:125–142. doi:10.1016/0022-1694(94)02604-A

Sofer, Z., and J.R. Gat. 1975. Isotope composition of evaporating brines: Effect of isotopic activity ratio in saline solutions. Earth Planet. Sci. Lett. 26:179–186. doi:10.1016/0012-821X(75)90085-0

Stewart, G.L. 1972. Clay–water interaction, behavior of ^3H and ^2H in adsorbed water, and isotope effect. Soil Sci. Soc. Am. Proc. 36:421–426. doi:10.2136/sssaj1972.03615995003600030018x

Striegl, R.G. 1988. Distribution of gases in the unsaturated zone at a low-level radioactive-waste disposal site near Sheffield, Illinois. Water-Resour. Invest. Rep. 88-4025. USGS, Urbana, IL.

Syvertsen, J.P., G.L. Cunningham, and T.V. Feather. 1975. Anomalous diurnal patterns of stem xylem water potentials in Larrea tridentata. Ecology 56:1423–1428. doi:10.2307/1934709

Tang, K.L., and X.H. Feng. 2001. The effect of soil hydrology on the oxygen and hydrogen isotopic compositions of plants' source water. Earth Planet. Sci. Lett. 185:355–367. doi:10.1016/S0012-821X(00)00385-X

Twining, J., D. Stone, C. Tadros, A. Henderson-Sellers, and A. Williams. 2006. Moisture isotopes in the biosphere and atmosphere (MIBA) in Australia: A priori estimates and preliminary observations of stable water isotopes in soil, plant and vapour for the Tumbarumba field campaign. Global Planet. Change 51:59–72. doi:10.1016/j.gloplacha.2005.12.005

Walker, G.R., P.H. Woods, and G.B. Allison. 1994. Interlaboratory comparison of methods to determine the stable isotope composition of soil water. Chem. Geol. 111:297–306. doi:10.1016/0009-2541(94)90096-5

Wang, L., K. Caylor, and D. Dragoni. 2009. On the calibration of continuous, high-precision $\delta^{18}O$ and δ^2H measurements using an off-axis integrated cavity output spectrometer. Rapid Commun. Mass Spectrom. 23:530–536. doi:10.1002/rcm.3905

Wang, L., K.K. Caylor, J.C. Villegas, G.A. Barron-Gafford, D.D. Breshears, and T.E. Huxman. 2010. Partitioning evapotranspiration across gradients of woody plant cover: Assessment of a stable isotope technique. Geophys. Res. Lett. 37:L09401. doi:10.1029/2010GL043228

Wang, L., S. Good, K. Caylor, and L.A. Cernusak. 2012. Direct quantification of leaf transpiration isotopic composition. Agric. For. Meteorol. 154–155:127–135. doi:10.1016/j.agrformet.2011.10.018

Warren, J., J. Brooks, M. Dragila, and F. Meinzer. 2011. In situ separation of root hydraulic redistribution of soil water from liquid and vapor transport. Oecologia 166:899–911. doi:10.1007/s00442-011-1953-9

Wassenaar, L.I., M.J. Hendry, V.L. Chostner, and G.P. Lis. 2008. High resolution pore water δ^2H and $\delta^{18}O$ measurements by H_2O(liquid)–H_2O(vapor) equilibration laser spectroscopy. Environ. Sci. Technol. 42:9262–9267. doi:10.1021/es802065s

Webster, C.R., and A.J. Heymsfield. 2003. Water isotope ratios D/H, 18O/16O, 17O/16O in and out of clouds map dehydration pathways. Science 302:1742–1745. doi:10.1126/science.1089496

Welp, L.R., R.F. Keeling, H.A.J. Meijer, A.F. Bollenbacher, S.C. Piper, K. Yoshimura, et al. 2011. Interannual variability in the oxygen isotopes of atmospheric CO2 driven by El Niño. Nature 477:579–582. doi:10.1038/nature10421

West, A.G., S.J. Partrickson, and J.R. Ehleringer. 2006. Water extraction times for plant and soil materials used in stable isotope analysis. Rapid Commun. Mass Spectrom. 20:1317–1321. doi:10.1002/rcm.2456

White, J.W.C., E.R. Cook, J.R. Lawrence, and W.S. Broecker. 1985. The D/H ratios of sap in trees: Implications for water sources and tree ring D/H ratios. Geochim. Cosmochim. Acta 49:237–246. doi:10.1016/0016-7037(85)90207-8

Wingate, L., J. Ogée, M. Cuntz, B. Genty, I. Reiter, U. Seibt, et al. 2009. The impact of soil microorganisms on the global budget of $\delta^{18}O$ in atmospheric CO2. Proc. Natl. Acad. Sci. 106:22411–22415. doi:10.1073/pnas.0905210106

Wingate, L., U. Seibt, K. Maseyk, J. Ogée, P. Almeida, D. Yakir, et al. 2008. Evaporation and carbonic anhydrase activity recorded in oxygen isotope signatures of net CO2 fluxes from a Mediterranean soil. Global Change Biol. 14:2178–2193. doi:10.1111/j.1365-2486.2008.01635.x

Worden, J., D. Noone, K. Bowman, and T.E. Spect. 2007. Importance of rain evaporation and continental convection in the tropical water cycle. Nature 445:528–532. doi:10.1038/nature05508

Yakir, D., and L.D.L. Sternberg. 2000. The use of stable isotopes to study ecosystem gas exchange. Oecologia 123:297–311. doi:10.1007/s004420051016

Yakir, D., and X.-F. Wang. 1996. Fluxes of CO_2 and water between terrestrial vegetation and the atmosphere estimated from isotope measurements. Nature 380:515–517. doi:10.1038/380515a0

Yamanaka, T., and R. Shimizu. 2007. Spatial distribution of deuterium in atmospheric water vapor: Diagnosing sources and the mixing of atmospheric moisture. Geochim. Cosmochim. Acta 71:3162–3169. doi:10.1016/j.gca.2007.04.014

Yepez, E., D. Williams, R. Scott, and G. Lin. 2003. Partitioning overstory and understory evapotranspiration in a semiarid savanna woodland from the isotopic composition of water vapor. Agric. For. Meteorol. 119:53–68. doi:10.1016/S0168-1923(03)00116-3

Yoshimura, K., S. Miyazaki, S. Kanae, and T. Oki. 2006. Iso-MATSIRO, a land surface model that incorporates stable water isotopes. Global Planet. Change 51:90–107. doi:10.1016/j.gloplacha.2005.12.007

Yu, W., T. Yao, L. Tian, Y. Wang, and C. Yin. 2005. Isotopic composition of atmospheric water vapor before and after the monsoon's end in the Nagqu River basin. Chin. Sci. Bull. 50:2755–2760. doi:10.1360/982005-802

Zimmerman, U., D. Ehhalt, and K.O. Munnich. 1967. Soil-water movement and evapotranspiration: Changes in the isotopic composition of the water. In: Proceedings of the Symposium on Isotopes in Hydrology. Int. Atomic Energy Agency, Vienna. p. 567–585.